Journal of Magnetism and Magnetic Materials 392 (2015) 22–26

Contents lists available at ScienceDirect

Journal of Magnetism and Magnetic Materials

journal homepage: www.elsevier.com/locate/jmmm

Solvothermal synthesis of $CoFe_2O_4$ submicron compact spheres and tunable coercivity induced via low-temperature thermal treatment

Ling Zhou [a], Qiuyun Fu [a,*], Dongxiang Zhou [a,b], Fei Xue [a], Yahui Tian [a]

[a] School of optical and electronic information, Huazhong University of Science and Technology, Wuhan 430074, PR China
[b] State Key Laboratory of Material Processing and Die & Mold Technology, Huazhong University of Science and Technology, Wuhan 430074, PR China

ARTICLE INFO

Article history:
Received 24 February 2015
Received in revised form
27 April 2015
Accepted 28 April 2015
Available online 29 April 2015

Keywords:
$CoFe_2O_4$
Compact spheres
Tunable coercivity
Thermal treatment
Exchange interactions

ABSTRACT

Compact $CoFe_2O_4$ submicron spheres were successfully prepared by a typical solvothermal synthesis method using potassium acetate as protective agent. The as-prepared spheres exhibited the onset of superparamagnetism. The saturation magnetization (M_s), remanent magnetization (M_r), coercivity (H_c) and remanence ratio R (M_r/M_s) were 46.79 emu/g, 0.84 emu/g, 18.4 Oe and 0.018, respectively. Followed by thermal treatment at 250–600 °C, the annealed spheres exhibited a sharp increment in coercivity without significant growth in crystal size. The coercivity of the sample annealed at 250 °C was 597.5 Oe and the sample annealed at 600 °C was increased to 1371.7 Oe. The probable mechanism of the increment in coercivity was suggested to be induced by the enhanced exchange interactions as the organics degraded in thermal treatment.

1. Introduction

In recent years, the research of spinel cobalt ferrite ($CoFe_2O_4$, abbreviated as CFO) particles has aroused widespread interest because of their excellent magnetic and electrical properties [1]. These particles can be used in many fields, such as magnetic recording [2–4], magnetic targeting technology in biology and medicine [5,6], magnetic fluid [7], radar absorbing stealth technology [8,9] and photocatalytic technology [10]. Many methods have been used to prepare these ferrites, for instance, sonochemical preparation [11], sol–gel method [12], microwave method [13], co-precipitation route [14,15], hydrothermal synthesis [16], solvothermal synthesis [8,9,17]. Among these methods, solvothermal synthesis has been widely used since Deng and his group had firstly prepared monodisperse ferrite microspheres in 2005 [17]. Researchers prepared various ferrites shaped in spheres [17], rugbies [9], nanosheets [18], and nanobelts [19] with compact [17], hollow [20] and porous structure [21]. These ferrite particles, however, are actually nanocrystalline clusters, when there is no restriction functional surfactant, these nanocrystals will grow up and aggregate together, form polycrystalline particles in an isotropic way. This growth model is called “oriented aggregation” [22]. Consequently, owing to their nanocrystalline features, these particles exhibit lower coercivity or even superparamagnetism, as compared to bulk samples.

Coercivity (H_c) is an important parameter in particular applications, in order to reach the maximum energy product $(BH)_{max}$, many authors report tuning the H_c through capping [23], mechanical milling treatment [24] and thermal annealing [25,26] of the grains. As thermal annealing treatment can easily modify grain crystalline and ferrite particle size, the H_c values can be easily tuned. The strong dependence on particle size of *Hc* of ferro- and ferrimagnetic solids has been widely reported: H_c firstly dramatically increases with the increasing particle size from a size (D_{sp}) [27] defined by the super-paramagnetic effect [28] to a“single domain” size (D_{crit}) [29,30], and gently increases until the particle size increases to an evolution of the monodomain structure towards a multidomain one, it then decreases. Therefore, in this paper, we attempt to utilize proper thermal treatment to promote the crystallinity of particles made by solvothermal synthesis method, in order to prepare monodisperse, size-controllable spheres with tunable H_c values, to fit specific applications.

2. Experimental section

CFO spinel ferrite submicron spheres were synthesized by a typical solvothermal [17] method. 0.01 mol $FeCl_3 \cdot 6H_2O$ (2.703 g), 0.005 mol $CoCl_2 \cdot 6H_2O$ (1.19 g) and 0.05 mol potassium acetate (KAc, 4.907 g) were dissolved in ethylene glycol (150 mL) and stirred vigorously for 4 h to form a homogeneous brown solution. Then the solution was poured into a Teflon-lined stainless-steel autoclave (180 mL capacity). The autoclave was heated to and

* Corresponding author. Fax: +86-27-87558482.
E-mail address: fuqy@mail.hust.edu.cn (Q. Fu).

http://dx.doi.org/10.1016/j.jmmm.2015.04.114
0304-8853/

maintained at 200 °C for 10 h, and naturally cooled to room temperature. The black powders were washed with ethanol several times and dried at 80 °C for 6 h. The as-prepared powders (S0) were then annealed at different temperatures from 250 to 600 °C (marked as S250–S600) with a heating rate of 250 °C/h and maintained for 2 h.

X-ray powder diffraction (XRD) of the powders was carried out on a Bruker D8-advance X-ray diffract meter with graphite-monochromatized Cu Kα radiation ($\lambda = 1.54056$ Å). Thermogravimetric (TG) and Differential Scanning Calorimetry (DSC) analysis of the as-prepared powders were carried out on a Netzsch STA449F3 simultaneous thermal analyzer in air with a heating rate of 10 °C/min. The morphology and the inner formation of the particles were determined at Philips CM12/STEM transmission electron microscope (TEM). The size of the submicron spheres was tested using Horiba dynamic light scattering particle size analyzer (DLS) LB-550. And the magnetic studies were carried out by using Lakeshore 7404 vibrating sample magnetometer (VSM) at room temperature.

3. Results and discussion

3.1. Structural analysis

Fig. 1 shows the XRD patterns of the samples of S0 and the annealed samples S250–S600. The diffraction peaks and relative intensities of all samples match well with a cubic spinel structure (JCPDS 01-1121, space group: Fd − 3m). However, the considerable broadening of all diffraction peaks of the samples suggests that the sizes of cobalt ferrite crystals are expected to be at a nano level. As the anneal temperature below 500 °C, the peak intensity slightly increases with the raise of anneal temperature, which indicates a tiny improvement in crystallinity. While the anneal temperature rose to 600 °C, there is a definite increase of the major peaks, indicating a larger grain size of cobalt ferrite crystals. The nanocrystals' approximate diameter which calculated by Scherrer formula are inserted in Fig. 1 too. Besides S500 and S600, the crystal size of the other samples are about 10–11 nm, near the superparamagnetic effect critical size (D_{sp}) [27] below which a spontaneous flip in magnetization occurs due to thermal effects. The blocking temperature, which is defined as the temperature at which the relaxation time is equal to the experimental measuring time, and often believed as the ferri- or ferromagnetic (FM) to superparamagnetic (SPM) transition temperature of the nanoparticles, depends on the particle size. The blocking temperature of CFO with 11 nm is reported to be 245 K [31], so that the as-prepared powders is expect to exhibit superparamagnetic features at room temperature.

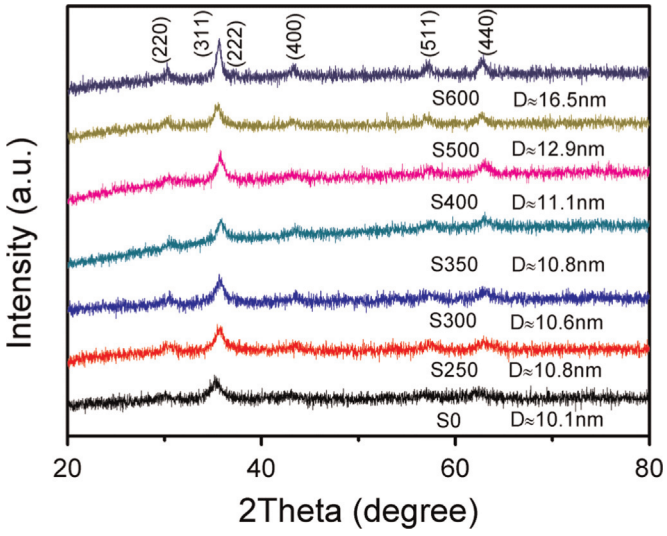

Fig. 1. X-ray diffractograms of the as-prepared powders S0 and the powders annealed at 250–600 °C.

3.2. Morphological characteristics and formation mechanism discussion

Fig. 2(a) shows the TEM image of as-prepared Co ferrite submicron spheres S0, the diameters of the spheres are in the range of 150–400 nm. Fig. 2(b) shows the higher magnification TEM image of a CFO sphere. The inset of Fig. 2(b) shows the boxed region of the edge. It shows that the spheres are constructed with tiny nanocrystallites with an average diameter of about 10 nm, which is close to the value calculated by Scherrer formula. It can be also clearly indicated that there existed many interspaces between the nanocrystallites. However, the spheres, unlike the hollow spheres prepared by other protective agents such as NaAc and PEG, are of compact structure on a macro level. Fig. 2(c) shows the TEM image of a sphere annealed at 600 °C, the inset shows the boxed region of the edge, too. There is an obvious increment in crystal size, and it worth mentioned that the crystals are overlapped without evident gaps between each other, indicating tight cohesion among those nanocrystals. Fig. 2(d) is the corresponding selected area electron diffraction (SAED) pattern of S600, suggesting that the CFO spheres are polycrystalline. The diffraction rings are corresponding to the (2 2 0), (3 1 1), (4 0 0), (4 2 2), (5 1 1) and (4 4 0) planes of CFO [32], which match the results of the XRD analysis.

Fig. 3(a) and (b) shows the particle size distribution of S0 which were obtained from TEM Fig. 2(a) and measured by the DLS particle size analyzer, respectively. From the DLS results, the particle size is in Gaussian distribution with the central of 258 nm, which is slightly lower than the results of statistical data from TEM images. The differences could be originated from the sedimentation of the big particles during DLS measurement, as well as the statistical error because of the small amount of spheres in the TEM image.

The formation mechanism of CFO nanoparticles and compact spheres may be as follows. At the beginning, the reactant mixtures of $FeCl_3 \cdot 6H_2O$, $CoCl_2 \cdot 6H_2O$, and KAc existed with their molecular form in the reacting system. As the reaction temperature rose up, the crystalline water of $FeCl_3 \cdot 6H_2O$ and $CoCl_2 \cdot 6H_2O$ was released and formed to numerous microreactors. KAc, owing to its hydrophilic group, would aggregate around these microreactors and exchanged their cations with ferric chloride and cobalt chloride to form ferrous acetate and cobalt acetate. Then, a dynamic competition between the breakage of Fe^{3+}–COO– bonds and the formation of Fe^{3+}–OH– bonds was established under the alkaline environment [33]. While a portion of Fe^{3+} were reduced to Fe^{2+} in the ethylene glycol, $Fe(OH)_3$ transformed to Fe_3O_4 precipitates, finally Co^{2+} substituted a portion of Fe^{2+} and formed to $CoFe_2O_4$ nanocrystals. While in the random aggregation procedure, it was different from the mechanism of hollow spheres synthesized in Ref. [20], the absence of PEG or oleic acid resulted none oil drops in water microreactors, resulted the formation of compact spheres. It is verified that these compact spheres were more stable than the hollow ones in our preparation of core–shell structured multiferroic composites.

Both the literature [17] and our work indicate that KAc plays an important role in ferrite formation. In this procedure, relative amount of KAc is needed. The minimum mole ratio of Fe^{3+} and Ac^- is 1:4. In our preparation, the solution of 0.01 mol $FeCl_3$ and 0.005 mol $CoCl_2$ need at least 0.04 mol KAc, below which the products cannot be synthesized. In fact, our attempt of adding less

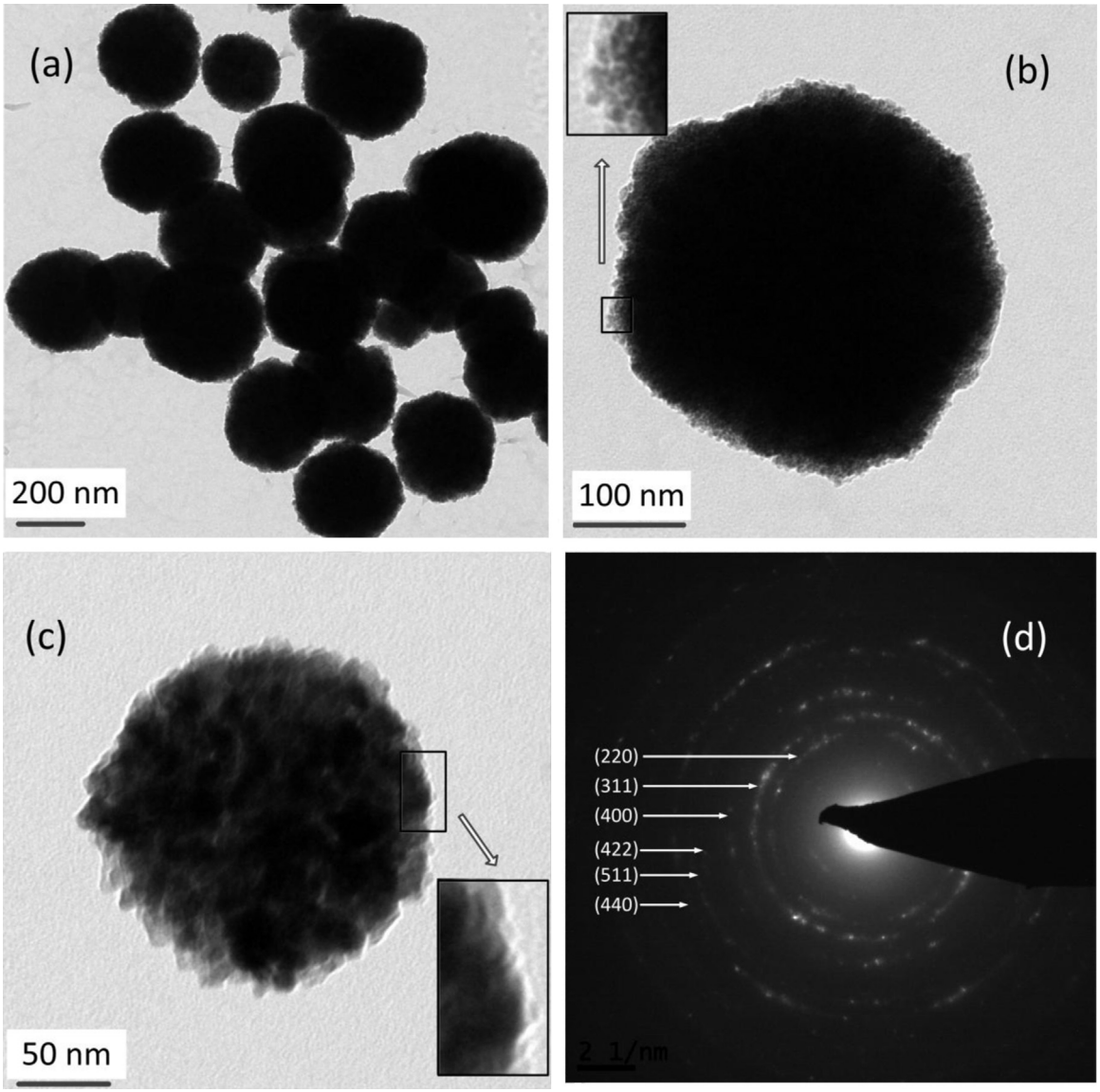

Fig. 2. (a) TEM image of submicron spheres S0, (b) TEM image of a sphere of S0, the inset is the boxed region of the edge, (c) TEM image of a sphere of S600, the inset is the boxed region of the edge and (d) SAED image of the S600 nanocrystals.

KAc (0.025 mol) was failed. In contrast, if more KAc is added, more and smaller microreactors would generate, thus lead to the decrease in sphere diameters. Similar results have been reported in Wang's work [34]. Furthermore, the alkaline environment provided by KAc is also the kay element in the formation of cobalt ferrite. It is suggested that the role of NaAc and NH_4Ac [34] is similar, except the different PH values caused by different cations.

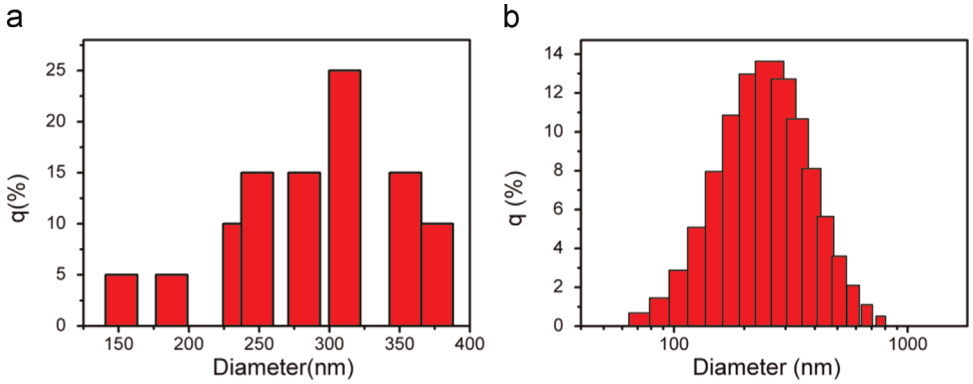

Fig. 3. The particle size distribution of S0, (a) obtained from TEM figure, and (b) obtained from DLS.

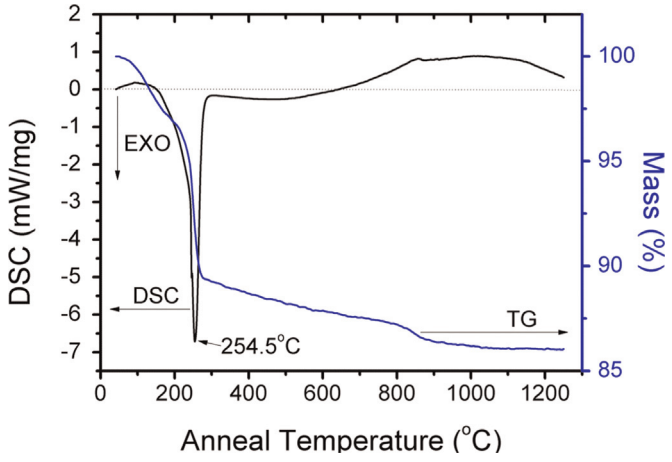

Fig. 4. TG–DTA curve of as-prepared powders S0.

3.3. Thermal analysis

The result of TG–DSC of S0 is shown in Fig. 4. The endothermic peak around 100 °C in the DTA curve corresponded to the evaporation of volatiles (H_2O, ethanol, etc.), and the exothermic peak at 254.5 °C corresponded to the decomposition of inorganic salts and the degradation of organics. The sharp decline of TG curve below 300 °C also indicated the degradation of inorganic and organic materials, which is corresponded to the DSC curve. Both the TG and DSC curves indicates that though the spheres are washed with ethanol several times, the organics containing of ethylene glycol and acetate salt still exist between the nanocrystals in the interior of spheres. The exothermic procedure maintained until the temperature increased to about 650 °C, indicating there is no significant grain growth or any phase transition, as was shown in XRD spectrum.

3.4. Magnetic properties

The RT magnetic hysteresis loops of S0 and annealed samples S250–S600 are shown in Fig. 5, the measured parameters obtained from those hysteresis loops are shown in Table 1. For S0, the M_s and M_r are 46.79 and 0.84 emu/g, and the H_c and remanence ratio R (M_r/M_s) are only 18.4 Oe and 0.018, respectively. However, the H_c values increases sharply even at a relative low anneal temperature

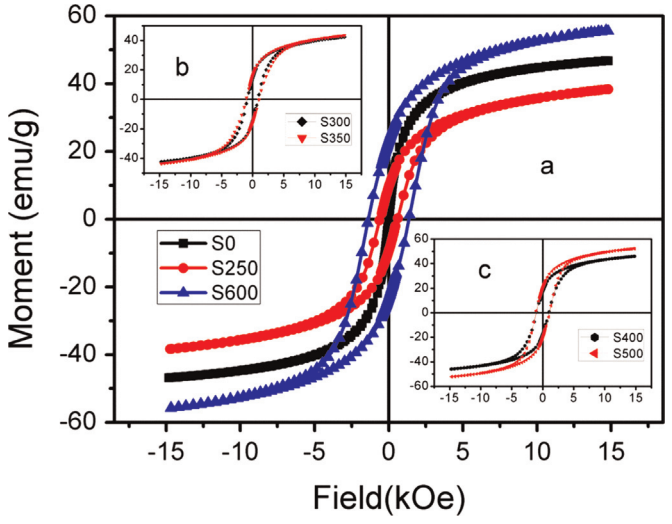

Fig. 5. *M–H* loops of (a) the as-prepared powders S0, S250 and S600 (b) S300 and S350 (c) S400 and S500.

Table 1
The measured parameters of S0 and annealed samples S250–S600.

Sample	Anneal temperature (°C)	H_c (Oe)	M_s (emu/g)	M_r (emu/g)	R
S0	Unannealed	18.4	46.79	0.84	0.018
S250	250	597.5	38.34	9.47	0.25
S300	300	860.0	42.39	14.74	0.35
S350	350	1009.3	43.51	15.93	0.37
S400	400	1046.1	45.92	17.50	0.38
S500	500	1106.2	52.25	20.26	0.39
S600	600	1371.7	55.75	23.21	0.42

range from 250 °C (597.5 Oe) to 350 °C (1009.3 Oe). For clearer presentation of the parameters' variation with anneal temperature, Fig. 6 shows the H_c and R of all samples as functions of anneal temperature, and the inset shows the measured M_s and M_r as functions of anneal temperature. As the anneal temperature rise up, the H_c and R first increase significantly at the range of 250–300 °C and remain stable at the range of 300–500 °C. While the temperature rise up to 600 °C, there is another increase of these two values. The H_c and R are 1371.7 Oe and 0.42 respectively, which are greatly higher than those of unannealed sample S0. There is a continues growth in M_r, however, the growth is slow down as the anneal temperature changes from 300 °C to 600 °C. The variation of M_s is different from the other parameters; it is decreased from 46.79 emu/g to the minimum 38.34 emu/g at 250 °C, and then increases and reaches 55.75 emu/g at 600 °C.

It is reported that the magnetic behavior of assembly spheres varies with the particle size and shape of the nanoparticles, and is also strongly affected by inter-particle interactions [35–37]. In our work, the size of nanocrystals is slightly changed as the anneal temperature increases from 250 °C to 500 °C, so it is suggest that the main reason for the great differences in their properties lies in the different extent of inter-particle interactions. For the unannealed sample S0, the covered organics, as mentioned above, have hampered the nanocrystal aggregation, led to the predominance of dipole–dipole interactions and the formation of ideal non-interacting system. Together with the nano crystal size, S0 exhibited room temperature superparamagnetic property. As the organics removed in thermal treatment, strong exchange interactions among particles tended to compensate the dipolar interactions, caused an increase in the anisotropy barriers, thus hampered the superparamagnetic relaxation, and resulted in the SPM–FM transition with sharply enhancements in coercivity and remanent magnetization. Similar phenomena were reported in many magnetic fluid and inter-particle interactions literatures, in which the magnetic nanoparticles were coated with surfactants

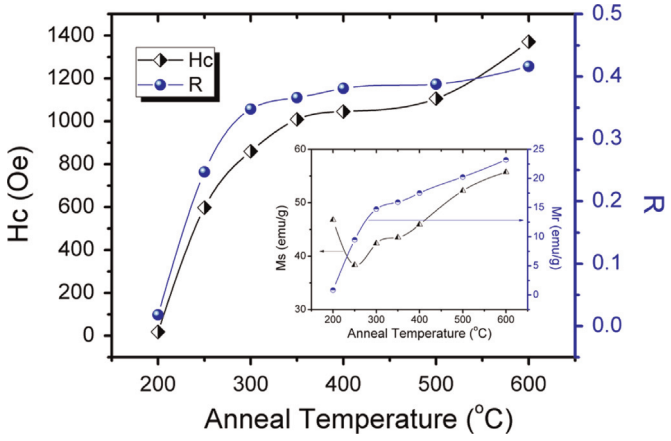

Fig. 6. The H_c and R as functions of annealed temperature, the inset shows the M_s and M_r as functions of annealed temperature.

[38,39] or embedded in a crystalline [40], polymers [41] or amorphous matrix [35,36]. When the anneal temperature increases from 350 °C to 500 °C, no additional organics were removed but tiny increase in nanocrystal diameter was promoted, which led to the gradual improvement in the magnetic properties. While the anneal temperature increased to 600 °C, there was an obvious growth in nanocrystal diameter, however, the diameter was still lower than the critical size of 40 nm [29,30] for single-domain to multidomain transition behavior of cobalt ferrite, beyond which the H_c will decrease, as reported in many literatures [25–27].

The changes of the saturation magnetization for the annealed samples could be attributed to the variation of surface effects during the thermal treatment. Haneda and Morrish [42,43] have reported the particles that made of nanocrystals were consist of a core with the usual spin arrangement and a boundary surface layer with atomic moments inclined to the direction of the net magnetization. The surface effects exist in these particles is the origin of a noncollinear structure that led to the reduction of the saturation magnetization. For our work, as the organics were removed at 250 °C, the increase in effective surfaces would lead to more noncollinear structure and result in the reduction of M_s. However, as the anneal temperature raised, the agglomeration of the nano crystals would reduce the effective surfaces and thus give rise to the subsequent improvement in M_s.

4. Conclusions

In conclusion, we have prepared $CoFe_2O_4$ submicron spheres by a typical solvothermal synthesis method using potassium acetate as protective agent. The spheres were more compact than those of using sodium acetate and PEG as protective agent. In addition, the probable mechanism of the formation of compact spheres was discussed. The as-prepared spheres exhibited proximately superparamagnetic properties with the M_s, M_r, H_c and remanence ratio R were 46.79 emu/g, 0.84 emu/g, 18.36 Oe and 0.018, respectively. Followed by thermal treatment at 250–600 °C, the annealed spheres exhibited a significant increment in coercivity without obvious growth in crystal size. The increment in coercivity was suggested to be induced by the stronger exchange interactions as the degradation of organics in thermal treatment.

Acknowledgments

The authors acknowledge the assistance by the Analytical and Testing Center of Huazhong University of Science and Technology. This work is financially supported by the National Nature Science Foundations of China under Grant no. 60871017 and the National High Technology Research and Development Program of China (863 Program) under Grant no. 2013AA030903.

References

[1] M.J. Iqbal, M.R. Siddiquah, J. Alloy. Compd. 453 (2008) 513–518, http://dx.doi.org/10.1016/j.jallcom.2007.06.105.
[2] S.H. Yu, M. Yoshimura, Adv. Funct. Mater. 12 (2002) 9–15, http://dx.doi.org/10.1002/1616-3028(20020101)12:1 < 9::AID-ADFM9 > 3.0.CO;2-A.
[3] N.A. Frey, S. Peng, K. Cheng, S.H. Sun, Chem. Soc. Rev. 38 (2009) 2532–2542, http://dx.doi.org/10.1039/b815548h.
[4] J.G. Lee, J.Y. Park, Y.J. Oh, C.S. Kim, J. Appl. Phys. 84 (1998) 2801, http://dx.doi.org/10.1063/1.368393.
[5] W.R. Zhao, J.L. Gu, L.X. Zhang, H.R. Chen, J.L. Shi., J. Am. Chem. Soc. 127 (2005) 8916–8917, http://dx.doi.org/10.1021/ja051113r.
[6] F. Caruso, M. Spasova, A. Susha, M. Giersig, R.A. Caruso., Chem. Mater. 13 (2001) 109–116, http://dx.doi.org/10.1021/cm001164h.
[7] N. Moumen, M.P. Pileni, J. Phys. Chem. 100 (1996) 1867–1873.
[8] R.L. Ji, C.B. Cao, Z. Chen, H.Z. Zhai, J. Bai, J. Mater. Chem. C 2 (2014) 5944, http://dx.doi.org/10.1039/c4tc00167b.
[9] Sl Zhang, Q.Z. Jiao, Y. Zhao, H.S. Li, Q. Wu, J. Mater. Chem. A 2 (2014) 18033–18039, http://dx.doi.org/10.1039/C4TA04286G.
[10] X. Feng, G.Y. Mao, F.X. Bu, X.L. Cheng, D.M. Jiang, J.S. Jiang, J. Magn. Magn. Mater. 343 (2013) 126–132, http://dx.doi.org/10.1016/j.jmmm.2013.05.001.
[11] K.V.P.M. Shafi, A. Gedanken, R. Prozorov, J. Balogh, Chem. Mater. 10 (1998) 3445–3450, http://dx.doi.org/10.1021/cm980182k.
[12] I.H. Gul, A. Maqsood, J. Alloy. Compd. 465 (2008) 227–231, http://dx.doi.org/10.1016/j.jallcom.2007.11.006.
[13] Y. Köseog˘lu, A. Baykal, F. Gözüak, H. Kavas, Polyhedron 28 (2009) 2887–2892, http://dx.doi.org/10.1016/j.poly.2009.06.061.
[14] X.H. Yang, X. Wang, Z.D. Zhang, J. Cryst. Growth 277 (2005) 467–470, http://dx.doi.org/10.1016/j.jcrysgro.2005.02.004.
[15] G. Jian, D.X. Zhou, J.Y. Yang, H. Shao, F. Xue, Q.Y. Fu, J. Eur. Ceram. Soc. 33 (2013) 1155–1163, http://dx.doi.org/10.1016/j.jeurceramsoc.2012.11.012.
[16] L.J. Zhao, H.J. Zhang, Y. Xing, S.Y. Song, S.Y. Yu, W.D. Shi, X.M. Guo, J.H. Yang, Y. Q. Lei, F. Cao, J. Solid State Chem. 181 (2008) 245–252, http://dx.doi.org/10.1016/j.jssc.2007.10.034.
[17] H. Deng, X.L. Li, Q. Peng, X. Wang, J.P. Chen, Y.D. Li, Angew. Chem.-Int. Ed. 44 (2005) 2782–2785, http://dx.doi.org/10.1002/anie.200462551.
[18] A.G. Yan, X.H. Liu, G.Z. Qiu, N. Zhang, R.R. Shi, R. Yi, M.T. Tang, R.C. Che, Solid State Commun. 144 (2007) 315–318, http://dx.doi.org/10.1016/j.ssc.2007.08.039.
[19] L.J. Zhao, Q. Jiang, Mater. Lett. 64 (2010) 677–679, http://dx.doi.org/10.1016/j.matlet.2009.12.036.
[20] Q. Liu, L.F. Lai, X.J. Fu, F.P. Zhu, J.H. Sun, H.R. Rong, M.Y. He, Q. Chen, Z. Xu, J. Mater. Sci. 42 (2007) 10113–10117, http://dx.doi.org/10.1007/s10853-007-2075-y.
[21] A.G. Yan, X.H. Liu, R. Yi, R.R. Shi, N. Zhang, G.Z. Qiu, J. Phys. Chem. C 112 (2008) 8558–8563, http://dx.doi.org/10.1021/jp800997z.
[22] B.P. Jia, L. Gao, Cryst. Growth Des. 8 (2008) 1372–1376, http://dx.doi.org/10.1021/cg070300t.
[23] M.V. Limaye, S.B. Singh, S.K. Date, D. Kothari, V.R. Reddy, Ay Gupta, V.T. Sathe, R.J. Choudhary, S.K. Kulkarni, J. Phys. Chem. B 113 (2009) 9070–9076, http://dx.doi.org/10.1021/jp810975v.
[24] A.S. Ponce, E.F. Chagas, R.J. Prado, C.H.M. Fernandes, A.J. Terezo, E. Baggio-Saitovitch, J. Magn. Magn. Mater. 344 (2013) 182–187, http://dx.doi.org/10.1016/j.jmmm.2013.05.056.
[25] W.S. Chiu, S. Radiman, R. Abd-Shukor, M.H. Abdullah, P.S. Khiew, J. Alloy. Compd. 459 (2008) 291–297, http://dx.doi.org/10.1016/j.jallcom.2007.04.215.
[26] Z.L. Wang, X.J. Liu, M.F. Lv, P. Chai, Y. Liu, X.F. Zhou, J. Meng, J. Phys. Chem. C 112 (2008) 15171–15175, http://dx.doi.org/10.1021/jp802614v.
[27] K.M. Krishnan, A.B. Pakhomov, Y. Bao, P. Blomqvist, Y. Chun, M. Gonzales, K. Griffin, X. Ji, B.K. Roberts, J. Mater. Sci. 41 (2006) 793–815, http://dx.doi.org/10.1007/s10853-006-6564-1.
[28] C.P. Bean, J. Appl. Phys. 26 (1955) 1381, http://dx.doi.org/10.1063/1.1721912.
[29] C.N. Chinnasamy, B. Jeyadevan, K. Shinoda, K. Tohji, D.J. Djayaprawira, M. Takahashi, R. Justin Joseyphus, A. Narayanasamy, Appl. Phys. Lett. 83 (2003) 2862, http://dx.doi.org/10.1063/1.1616655.
[30] Diandra L. Leslie-Pelecky, Reuben D. Rieke, Chem. Mater. 8 (1996) 1770–1783.
[31] B.G. Toksha, Sagar E. Shirsath, S.M. Patange, K.M. Jadhav, Solid State Commun. 147 (2008) 479–483, http://dx.doi.org/10.1016/j.ssc.2008.06.040.
[32] D.K. Lee, Y.S. Kang, Colloids Surf. A: Physicochem. Eng. Asp. 257–258 (2005) 237–241, http://dx.doi.org/10.1016/j.colsurfa.2004.07.034.
[33] Q. Wang, A.B. Wu, L.X. Yu, Z.L. Liu, W. Xu, H. Yang, J. Phys. Chem. C 113 (2009) 19875–19882, http://dx.doi.org/10.1021/jp909049b.
[34] J.Y. Wang, F.L. Ren, R. Yi, A.G. Yan, G.Z. Qiu, X.H. Liu, J. Alloy. Compd. 479 (2009) 791–796, http://dx.doi.org/10.1016/j.jallcom.2009.01.059.
[35] D. Peddis, C. Cannas, A. Musinu, G. Piccaluga, Chem.-A Eur. J. 15 (2009) 7822–7829, http://dx.doi.org/10.1002/chem.200802513.
[36] D. Peddis, C. Cannas, A. Musinu, G. Piccaluga, J. Phys. Chem. C 112 (2008) 5141–5147, http://dx.doi.org/10.1021/jp076704d.
[37] D. Roy, P.S. Anil Kumar, J. Appl. Phys. 106 (2009) 073902, http://dx.doi.org/10.1063/1.3213341.
[38] S. Odenbach, J. Phys.: Condens. Matter 16 (2004) R1135–R1150, http://dx.doi.org/10.1088/0953-8984/16/32/R02.
[39] M.S. Seehra, H. Shim, P. Dutta, A. Manivannan, J. Bonevich, J. Appl. Phys. 97 (2005) 10J509, http://dx.doi.org/10.1063/1.1854911.
[40] A. Corrias, M.F. Casula, A. Falqui, G. Paschina, Chem. Mater. 16 (2004) 3130, http://dx.doi.org/10.1021/cm049796h.
[41] Sufi R. Ahmed, S.B. Ogale, G.C. Papaefthymiou, R. Ramesh, P. Kofinas, Appl. Phys. Lett. 80 (2002) 1616, http://dx.doi.org/10.1063/1.1456258.
[42] K. Haneda, A.H. Morrish, J. Appl. Phys. 63 (1988) 4528, http://dx.doi.org/10.1063/1.340197.
[43] A.H. Morrish, K. Haneda, J. Magn. Magn. Mater. 35 (1983) 105–113.